NEW MAPS OF MAJOR OXIDES AND MG # OF THE LUNAR SURFACE FROM ADDITIONAL GEOCHEMICAL DATA OF CHANG'E-5 SAMPLES AND KAGUYA MULTIBAND IMAGER DATA.

Liang Zhang[1], Xubing Zhang[2], Maosheng Yang[1], Xiao Xiao[1], Denggao Qiu[3], Jianguo Yan[3], Long Xiao[1], and Jun Huang[1,4*], [1]State Key Laboratory of planetary processes and mineral resources, School of Earth Sciences, China University of Geosciences (Wuhan), Wuhan 430074, China, liangz@cug.edu.cn, [2]School of Geography and Information Engineering, China University of Geosciences, Wuhan 430078, China, [3]State Key Laboratory of Information Engineering in Surveying, Mapping and Remote Sensing, Wuhan University, Wuhan 430070, China, [4]Chinese Academy of Sciences Center for Excellence in Comparative Planetology, Hefei 230026, China.

Introduction: In the past, global maps of major oxides and magnesium number (Mg #) of the lunar surface had been derived from spectral data of remote sensing images with "ground truth" geochemical information from Apollo and Luna samples. These compositional maps provide insights into the chemical variations of different geologic units, thus the regional and global geologic evolution. In this study, we produced new maps of five major oxides (i.e., Al_2O_3, CaO, FeO, MgO, and TiO_2) and Mg # with imaging spectral data of KAGUYA multiband imager (MI) with the one- dimensional convolutional neural network （1D-CNN） algorithm, taking advantage of recently acquired geochemical information of China' s Chang' E-5 (CE-5) samples. The 1D-CNN algorithm generally performs better in describing the complex nonlinear relationship between spectra and chemical components. In addition, we present regions of mare domes in Mairan Dome (43.76°N, 49.90°W), and irregular mare patches (IMPs) in Sosigenes (8.34°N, 19.07°E) to demonstrate the geologic implications of these new maps. With the highest spatial resolution (~ 59 m / pixel), these new maps of five major oxides and Mg # will serve as an important guide in the future study of lunar geology.

Methods and datasets: The MI global mosaic covers the range from 65°N ~ 65°S on the lunar surface [1], with a high spatial resolution of ~ 59 m / pixel. We use eight bands (415 nm, 750 nm, 900 nm, 950 nm, 1001 nm, 1050 nm, 1250 nm, and 1550 nm) of the MI global mosaic to calculate the abundances of the five major oxides in this study. For the bench mark points, we included CE-5 samples [2-4], Apollo samples (except for Apollo 11, whose sampling site is not covered by the MI global mosaic), Luna samples, and in situ measurements of CE-3 rover [5-6]. In order to reduce the noise impact of MI data, we selected the average reflectance value of bench mark points in the 2×2 or 3×2 pixels to represent the "ground truth" geochemical information.

We used the 1D-CNN to build a nonlinear regression model to describe the relationship between measured oxide content and reflectivity of each sampling area. As shown in Figure 1, the 1D-CNN includes 4-layer convolution layer, 2-layer pooling layer and 1-layer full connected layer in this study. The input data of the network corresponds to the spectral reflectance values of 8 bands of MI multispectral data. Feature vectors are extracted by the convolution layer. Then, in order to avoid the overfitting problem, the size of the feature vector is compressed by the pooling layer. Then, the feature map is converted into a one-dimensional feature vector through the fully connected layer. Finally, the extracted features are converted into the corresponding sample chemical composition data (i.e., the predicted value of oxide content) through the linear activation function.

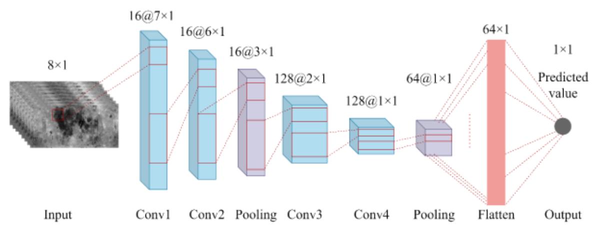

Figure 1. Regression model of lunar major oxides based on 1D-CNN.

Results: The global maps of five major oxides and Mg # are shown in Figure 2. From the perspective of the global, these oxides exhibit the characteristics of dichotomous distributions between the maria and the highlands.

We selected two compositionally interesting regions shown in this study (Figure 3 and Figure 4), including Mairan Domes (43.76°N, 49.90°W) and Sosigenes (8.34°N, 19.07°E). Then, by analyzing the inversion results of five major oxides to demonstrate the geologic implications of these new maps.

Conclusions: This study complements the data of the CE-5 sampling point based on the previous sampling point data and reports the new maps of five major oxides and Mg # on the moon of high spatial resolution (~ 59 m / pixel). By analyzing the major oxide content of lunar mare domes and IMPs in the study area, we found that there is a certain difference between the major oxide content of formation and lithology in the study area. Thus, these new maps of major oxides will serve as an important guide in the future study of lunar geology.

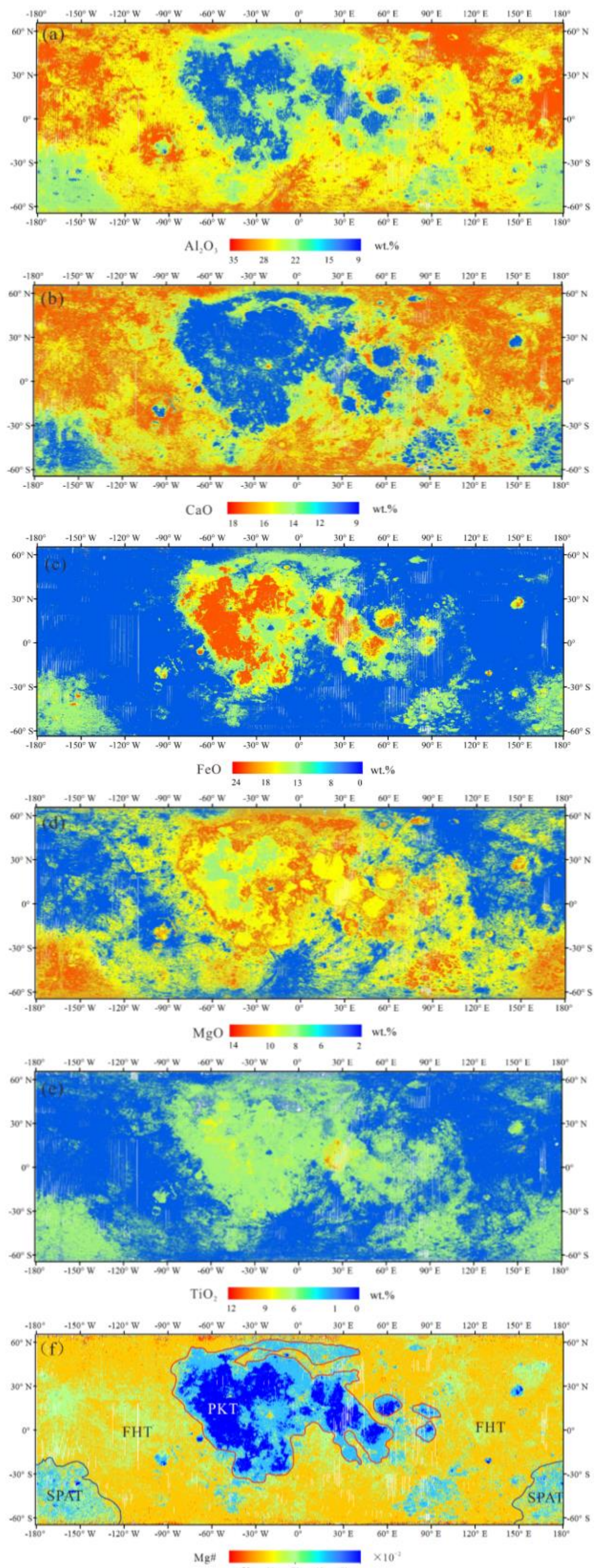

Figure 2. Maps of (a) Al_2O_3; (b) CaO; (c) FeO; (d) MgO; (e) TiO_2 abundances and (f) Mg #. The Mg # map highlights the approximate boundaries of three lunar geological terranes (PKT, FHT, and SPAT) (Jolliff et al., 2000)[7].

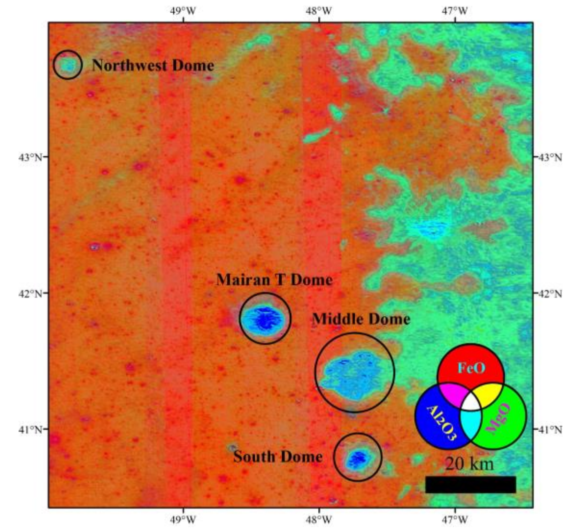

Figure 3. Color composite image of Mairan Domes. The red channel is FeO abundance (stretched from 0.50 to 31.10). The Green channel is MgO abundance (stretched from 1.48 to 13.81). The blue channel is Al_2O_3 abundance (stretched from 9.17 to 32.50).

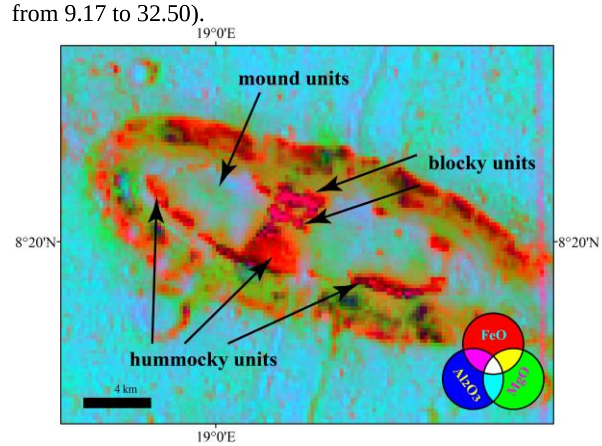

Figure 4. Color composite image of Sosigenes. The red channel is FeO abundance (stretched from 15.50 to 25.58). The Green channel is MgO abundance (4.31 to 9.43). The blue channel is Al2O3 abundance (7.52 to 17.12).

Acknowledgments: This study was supported by the National Natural Science Foundation of China (42273041) and Wuhan Science and Technology Plan Project-Application Basic Frontier Project (2019010701011403).

References: [1] Ohtake, M. et al. (2008) *EPS, 60*, 257-264. [2] Tian, H.C. et al. (2021) *Nature, 600*, 7887. [3] Li, C. et al. (2022) *NSR, 9(2)*, nwab188. [4] Zong, K. et al. (2022) *GCA, 335*, 284-296. [5] Zhang, J. et al. (2015) *the National Academy of Sciences of the United States of America, 112(17)*, 5342-7. [6] Ling, Z. et al. (2015) *Nature Communications, 6(1)*, 1–9. [7] Jolliff, B. L.et al. (2000) *JGR-P, 105 (E2)*, 4197–4216.